IEEE Access
Multidisciplinary | Rapid Review | Open Access Journal

Received March 28, 2019, accepted April 14, 2019, date of publication May 6, 2019, date of current version May 22, 2019.

Digital Object Identifier 10.1109/ACCESS.2019.2913041

Resource Allocation for Energy Harvesting-Powered D2D Communications Underlaying NOMA-Based Networks

BO CHEN, JUAN LIU, (Member, IEEE), XINJIE YANG, LINGFU XIE, AND YOUMING LI
College of Information and Electronic Engineering, Ningbo University, Ningbo 315211, China

Corresponding author: Bo Chen (chenbo3@nbu.edu.cn)

This work was supported in part by the National Natural Science Foundation of China (NSFC) under Grant 61601255, in part by the Natural Science Foundation of Zhejiang Province under Grant LQ18F010002, and Grant LY19F010003, in part by the K.C. Wong Magna Fund of Ningbo University, and in part by the Foundation of Ningbo University under Grant XYL19026.

ABSTRACT This paper investigates the resource allocation problem in device-to-device (D2D) communications underlaying a non-orthogonal multiple access (NOMA)-based cellular network with energy harvesting, where the energy harvesting-powered D2D communications share the downlink resources of the cellular network. To fully exploit the high-data-rate D2D links in this system, a two-phase framework is proposed for D2D users. In particular, the D2D users harvest energy from the base station (BS) in the first phase and then transmit their own information using the harvested energy in the second one. Meanwhile, the D2D communications could cause severe interference to cellular users (CUs) and hence probably ruin the SIC decoding order of the CUs. To deal with this issue, joint power allocation and time scheduling scheme is proposed to maximize the throughput of the D2D links while guaranteeing the quality of service (QoS) for each CU. Through rigorous derivation, the optimal power control and time scheduling parameters are analyzed to simplify the optimization problem formulation. The closed-form optimal solution is derived in some cases. In other cases, a gradient-based algorithm is employed to find an appropriate sub-optimal solution. The simulation results are demonstrated to validate the superiority of the proposed scheme over the conventional orthogonal multiple access (OMA) scheme.

INDEX TERMS D2D, NOMA, energy harvesting, resource allocation, cellular networks.

I. INTRODUCTION

The device-to-device (D2D) communications deployed in wireless cellular networks allow users in close proximity to communicate directly instead of via base stations (BSs), and have been considered as a promising way to alleviate the upcoming traffic pressure on core networks [1]–[3]. The D2D users can share the same spectrum resources with cellular users (CUs) under control of the cellular network, which can effectively improve the spectral efficiency. In general, the overlay and underlay spectrum sharing techniques are commonly used for D2D and cellular communication links [4]. With the overlay spectrum sharing, D2D users can only employ the idle spectrum that are not currently utilized by the CUs, whereas the underlay spectrum sharing technology allows D2D links to reuse the resource of the cellular links. It can further improve spectral efficiency at the cost of resulting in the co-channel interference between the D2D and cellular links. Therefore, it is important to investigate the resource allocation problems in D2D communications underlaying the cellular networks, which have been extensively studied in [5]–[7]. In [5], the authors proposed a power allocation algorithm to maximize the sum rate of D2D links, and guarantee the performance of the cellular link at the same time. Power allocation for both cellular and D2D links was studied to maximize the rate of the single D2D link in [6]. In [7], the authors studied the system with multiple cellular and D2D links.

Apart from invoking the D2D technique to improve the system spectral efficiency, non-orthogonal multiple access (NOMA) is also a promising technology to improve the spectral efficiency, on the standpoint of providing power dimension for multiple access [8], [9]. It is considered as a key

The associate editor coordinating the review of this manuscript and approving it for publication was Wenchi Cheng.

technology to meet the challenging requirements of the fifth generation (5G) wireless networks. With the aid of NOMA, multiple CUs are allowed to share the same sub-channels via different power levels, and successive interference cancellation (SIC) is adopted at the receivers for decoding [10]. In [11], the authors considered a general downlink NOMA transmission scenario in which the BS communicates with multiple randomly deployed CUs. The power allocation techniques were studied to ensure fairness among the downlink CUs under the constraints of instantaneous and average channel state information (CSI) in [12]. In [13], the authors developed a novel power allocation scheme in the downlink and uplink NOMA scenarios with two users while the strict quality of service (QoS) was guaranteed.

Recently, several approaches have been proposed to combine the D2D communications and NOMA technologies [14]–[17]. In [14], the authors proposed a full-duplex D2D-aided cooperative NOMA scheme to improve the system performance of the NOMA-weaker CU. The D2D users were grouped through the NOMA way in [15] to achieve a better D2D rate performance using sophisticated power control. A D2D aided cooperative relaying system with NOMA was considered in [16], where a power allocation strategy was introduced to achieve the maximum scaling capacity according to the signal-to-noise ratio (SNR) conditions. The power control and channel assignment problem for D2D communications underlaying a NOMA-based cellular network was investigated to maximize the sum rate of D2D pairs subject to the minimum rate requirements of the NOMA-based CUs in [17].

It is noted that the system throughput in D2D underlaying cellular networks is seriously limited by the battery lifetime budget of users. Hence, in order to prolong the network lifetime, energy harvesting from radio frequency has been applied to D2D underlaying cellular networks [18], [19]. In [18], joint time scheduling and power control was considered for a D2D underlaying cellular network, where the D2D transmitters were powered by energy harvested from the uplink transmission of CUs and the signal-interference-noise ratio (SINR) requirements of CUs were guaranteed. The resource allocation problem in a D2D underlaying NOMA-based cellular network was investigated in [19], where both CUs and D2D users harvested energy from the BS in the downlink and transmitted their information in the uplink. Both [18] and [19] considered the communication scenarios that the D2D pairs reused the uplink spectrum of the CUs for the transmission. In such cases, the BS performs the SIC decoding according to the uplink SINR of the CUs. When the D2D users reutilize the downlink spectrum with NOMA-enabled CUs, the SIC decoding at the receiver of each CU becomes complicated, since the excessive co-channel interference from the D2D link may change the relative SINR9 at each CU and probably destroy the original SIC decoding order of the CUs. How to protect the SIC decoding order of the CUs subject to the co-channel interference should be carefully considered.

Motivated by the above works, we consider a joint power control and time scheduling problem for the D2D pair underlaying NOMA-based cellular networks with energy harvesting. Our target is to maximize the throughput of the D2D communication while the minimum rate requirements of the CUs are strictly guaranteed. By power control and time scheduling, the D2D users can efficiently reuse the downlink spectrum of CUs without causing any trouble to CUs that employ NOMA and SIC decoding techniques. In particular, the contribution of this paper is three-fold:

- A joint power allocation and time scheduling problem is properly formulated to maximize the throughput of the D2D link while guaranteeing the minimum rate requirement for each CU.
- The corresponding resource optimization problem is mathematically solved. First, the optimal power control and time scheduling parameters are analyzed to simplify the optimization problem formulation through rigorous derivation. Second, the closed-form optimal solution is derived in some cases. In the other cases, a sub-optimal solution with low complexity by employing the gradient algorithm is obtained.
- The conventional orthogonal multiple access (OMA) scheme is provided as a benchmark. The simulation results show that the proposed scheme outperforms the OMA scheme.

The rest of this paper is organized as follows. In Section II, we introduce the system model and formulate the problem of joint power control and time scheduling. The formulated problem is analyzed and solved to find the optimal solution in Section III. In Section IV, the conventional OMA scheme is described. Section V presents the simulation results and the conclusions are drawn in Section VI.

II. SYSTEM MODEL AND PROBLEM FORMULATION

Consider a NOMA-based cellular network with one BS communicating with K CUs (U_i, $i \in \mathcal{K} = \{1, \cdots, K\}$). The CUs are uniformly distributed in a disc with radius D, and the BS is located in the center. There exists one pair of D2D users that can utilize the downlink spectrum resource of the CUs. We assume that all the users and the BS are equipped with one single antenna. A two-phase transmission framework with time interval of T seconds is adopted. The BS serves all the CUs by employing the NOMA-based scheme in both two phases, whereas the D2D transmitter (DTX) harvests energy from the BS in the first phase and communicates with the D2D receiver (DRX) during the second phase. The lengths of the two phases are denoted by τ_e and τ_t, respectively. The time intervals τ_e and τ_t should satisfy

$$\tau_e + \tau_t \leq T. \tag{1}$$

In this paper, we assume that the perfect CSI is available and constant during each framework. Define h_i, h_D, h_{B,D_t}, h_{B,D_r} and $h_{D,i}$ as the channel from the BS to the i-th CU, from the DTX to the DRX, from the BS to the DTX, from the BS to

the DRX, and from the DTX to the i-th CU, respectively. The background noise is modeled as the additive white Gaussian noise (AWGN) with zero mean and variance σ^2. Without loss of generality, we assume $|h_1| \geq |h_2| \geq \cdots \geq |h_K|$. Hence, based on the principle of the SIC process, the cellular user U_i can successfully decode and remove the interference from U_j for any $j > i$.

In the first phase, the composite transmit signal x_B^1 from the BS can be expressed as

$$x_B^1 = \sum_{k=1}^{K} \sqrt{\omega_k P_B} s_k, \tag{2}$$

where s_k is the transmit signal for U_k, P_B is the total transmit power of the BS, ω_k is the power allocation coefficient for U_k, and $\boldsymbol{\omega} = [\omega_1, \cdots, \omega_K]$ is the power allocation vector. We assume that the BS broadcasts the signal x_B^1 with its maximum transmit power P_B to maximize the spectrum efficiency, namely

$$\sum_{k=1}^{K} \omega_k = 1. \tag{3}$$

At the receiver side, following the principle of NOMA, each cellular user U_i can successfully decode the signal of U_j ($j > i$), treating the signals of $U_1, U_2, \cdots, U_{j-1}$ as interferences. Accordingly, the received SINR at U_i for decoding the signal s_j ($j > i$) is given by

$$SINR_{i,j}^1 = \frac{\omega_j |h_i|^2 \rho_B}{\sum\limits_{k=1}^{j-1} \omega_k |h_i|^2 \rho_B + 1}, \tag{4}$$

where $\rho_B = \frac{P_B}{\sigma^2}$ is the transmit signal-to-noise ratio (SNR) at the BS. Since $|h_i| > |h_j|$ ($i < j$), $SINR_{j,j}^1 < SINR_{i,j}^1$ holds for any $j > i$.

Meanwhile, the DTX harvests energy from the BS when it transmits with power P_B. The total amount of energy harvested by the DTX in the first phase can be calculated as

$$E_D^h = \tau_e \eta P_B |h_{B,D_t}|^2, \tag{5}$$

where η is the energy transformation efficiency.

In the second phase, the transmit signal x_B^2 from the BS can be accordingly expressed as

$$x_B^2 = \sum_{k=1}^{K} \sqrt{\alpha_k P_B} s_k, \tag{6}$$

where α_k is the power allocation coefficient for U_k, and $\boldsymbol{\alpha} = [\alpha_1, \cdots, \alpha_K]$ is the power allocation vector. Then $\boldsymbol{\alpha}$ should satisfy

$$\sum_{k=1}^{K} \alpha_k \leq 1, \quad \alpha_k \geq 0, \ \forall k \in \mathcal{K}. \tag{7}$$

At the same time, the DTX utilizes the harvested energy to transmit information with power p_D over the downlink spectrum. For the DTX, energy consumption should not exceed the harvested energy

$$\tau_e p_D^e + \tau_t p_D + \tau_t p_D^t \leq E_D^h, \tag{8}$$

where p_D^e and p_D^t denote the constant circuit power in the first and second phases. In practice, considering the fact that the circuits of signal processing and transmission are more complex than those of energy harvesting [19], we set $p_D^t > p_D^e$.

The received SINR at the DRX can be calculated as

$$SINR_D^2 = \frac{|h_D|^2 \rho_D}{\sum\limits_{k=1}^{K} \alpha_k |h_{B,D_r}|^2 \rho_B + 1}, \tag{9}$$

where $\rho_D = \frac{p_D}{\sigma^2}$ is the transmit SNR at the DTX. Meanwhile, each cellular user suffers interferences from the DTX and other cellular users. Similarly, when SIC is adopted with the same decoding sequence at each cellular user U_i, the received SINR for decoding the signal s_j ($j > i$) is expressed as

$$SINR_{i,j}^2 = \frac{|h_i|^2 \alpha_j \rho_B}{\sum\limits_{k=1}^{j-1} \alpha_k |h_i|^2 \rho_B + |h_{D,i}|^2 \rho_D + 1}. \tag{10}$$

To decode the signal s_j successfully, the received SINR at U_i should be no less than the received SINR at U_j itself, i.e., $SINR_{i,j}^2 \geq SINR_{j,j}^2 (j > i)$. From (10), we have

$$\frac{|h_{D,i}|^2 \rho_D + 1}{|h_i|^2} \leq \frac{|h_{D,j}|^2 \rho_D + 1}{|h_j|^2}, \quad K \geq j > i \geq 1. \tag{11}$$

Note that the inequalities in (11) can be equivalently expressed as

$$\frac{|h_{D,i}|^2 \rho_D + 1}{|h_i|^2} \leq \frac{|h_{D,i+1}|^2 \rho_D + 1}{|h_{i+1}|^2}, \quad K - 1 \geq i \geq 1. \tag{12}$$

According to the theory of Shannon capacity, we can obtain the achievable rates of U_i in the two phases, and the achievable rate of the D2D link in the second phase as

$$\begin{aligned} R_i^1 &= \log_2(1 + SINR_{i,i}^1), \\ R_i^2 &= \log_2(1 + SINR_{i,i}^2), \\ R_D^2 &= \log_2(1 + SINR_D^2), \end{aligned} \tag{13}$$

where the bandwidth is normalized. Meanwhile, the minimum rate requirements of the CUs should be guaranteed for both two phases, namely

$$R_i^1 \geq \gamma_i, \quad R_i^2 \geq \gamma_i, \ \forall i \in \mathcal{K}, \tag{14}$$

where γ_i denotes the target rate of U_i.

To maximize the throughput of the D2D communication under the constraint of the QoS for each CU, we can formulate a resource allocation problem as follows

$$\max_{\tau_e, \tau_t, \boldsymbol{\alpha}, \boldsymbol{\omega}, \rho_D} \ U_D = \tau_t R_D^2, \tag{15a}$$

$$\text{s.t. } (1), (3), (7), (8), (12), (14). \tag{15b}$$

Problem (15) is a non-convex optimization problem, since its objective and constraints are both non-convex functions of the

variables. To make it tractable, we then analyze the optimal solution to (15), and reformulate a simplified optimization problem just with variables ρ_D and τ_t in the next section.

III. ANALYTICAL FRAMEWORK

In this section, we first discuss the relationship among the variables so as to simplify the constraints of (15). Then, the original optimization problem (15) can be reformulated as an optimization problem just with ρ_D and τ_t being the variables. Finally, the optimal solution can be obtained in two different scenarios according to the feasible values of τ_t.

A. PROBLEM REFORMULATION

First, from (4) and (10), we can see that $R_i^1 > R_i^2$ for $\boldsymbol{\omega} = \boldsymbol{\alpha}$. Therefore, if $\boldsymbol{\alpha}^*$ satisfies $R_i^2 \geq \gamma_i$ for all $i \in \mathcal{K}$, we can set $\omega_1^* = 1 - \sum_{k=2}^{K} \omega_k^*, \omega_2^* = \alpha_2^*, \cdots, \omega_K^* = \alpha_K^*$, which means that $\boldsymbol{\omega}^*$ naturally satisfies $R_i^1 \geq \gamma_i$ for all $i \in \mathcal{K}$. Hence, the constraint (14) can be recast as

$$R_i^2 \geq \gamma_i, \quad \forall i \in \mathcal{K}. \tag{16}$$

Accordingly, the problem (15) can be equivalently written as

$$\max_{\tau_e, \tau_t, \boldsymbol{\alpha}, \rho_D} U_D = \tau_t R_D^2, \tag{17a}$$

$$\text{s.t. (1), (7), (8), (12), (16).} \tag{17b}$$

Next, we analyze the optimal solution to (17), and reformulate a simplified problem just with variables ρ_D and τ_t.

Theorem 1: The optimal solution of problem (17) can be obtained when the equalities in constraints (1) and (16) hold, namely

$$\tau_e^* + \tau_t^* = T, \tag{18}$$

$$R_i^{2*} = \gamma_i, \quad \forall i \in \mathcal{K}. \tag{19}$$

Proof: See Appendix A. ∎

From (19), the optimal power allocation vector $\boldsymbol{\alpha}$ can be obtained by the following theorem.

Theorem 2: The optimal $\boldsymbol{\alpha}^*$ can be derived as

$$\alpha_i^* = \frac{\sum_{j=1}^{i-1} \left\{ \left[\prod_{t=j+1}^{i-1} (1+\phi_t) \right] \phi_i \phi_j (\delta_j \rho_D^* + \theta_j) \right\} + \phi_i (\delta_i \rho_D^* + \theta_i)}{\rho_B}, \tag{20}$$

where $\phi_i = 2^{\gamma_i} - 1, \delta_i = \frac{|h_{D,i}|^2}{|h_i|^2}, \theta_i = \frac{1}{|h_i|^2}, \forall i \in \mathcal{K}$. Note that $\sum_{j=1}^{i-1} \left\{ \left[\prod_{t=j+1}^{i-1} (1+\phi_t) \right] \phi_i \phi_j (\delta_j \rho_D^* + \theta_j) \right\} = 0$ for $i = 1$, and $\prod_{t=j+1}^{i-1} (1+\phi_t) = 1$ for $j+1 > i-1$.

Proof: See Appendix B. ∎

Theorem 2 represents the relationship between the optimal α_i^* and ρ_D^*. Then, from *Theorem 2* and its proof, we can analyze the feasible region of variable ρ_D. By substituting (20), we define $H(\rho_D) = \sum_{i=1}^{K} \alpha_i = \frac{\sum_{j=1}^{K} \left\{ \left[\prod_{t=j+1}^{K} (1+\phi_t) \right] \phi_j (\delta_j \rho_D + \theta_j) \right\}}{\rho_B} = \bar{A}\rho_D + \bar{B}$, where $\bar{A} = \frac{\sum_{j=1}^{K} \left\{ \left[\prod_{t=j+1}^{K} (1+\phi_t) \right] \phi_j \delta_j \right\}}{\rho_B}$, and $\bar{B} = \frac{\sum_{j=1}^{K} \left\{ \left[\prod_{t=j+1}^{K} (1+\phi_t) \right] \phi_j \theta_j \right\}}{\rho_B}$. Due to the fact that $\phi_i > 0, \delta_i > 0, \theta_i > 0, \forall i \in \mathcal{K}$, we can easily conclude that $\bar{A} > 0, \bar{B} > 0$, and $H(\rho_D)$ increases linearly with ρ_D.

Remark 1: From the inequality (7), we have $\bar{A}\rho_D + \bar{B} \leq 1$, and equivalently

$$0 \leq \rho_D \leq \frac{1 - \bar{B}}{\bar{A}}. \tag{21}$$

Recall that Eq. (12) can be expressed as

$$(\delta_i - \delta_{i+1})\rho_D \leq \theta_{i+1} - \theta_i, \quad 1 \leq i \leq K-1. \tag{22}$$

This inequality (22) naturally holds if $\delta_i \leq \delta_{i+1}$. Otherwise, the power variable ρ_D satisfies $0 \leq \rho_D \leq \frac{\theta_{i+1} - \theta_i}{\delta_i - \delta_{i+1}}$.

Combing (21) and (22), we can further obtain

$$0 \leq \rho_D \leq \min\{\frac{1 - \bar{B}}{\bar{A}}, \min_{j \in \mathcal{I}} \frac{\theta_{j+1} - \theta_j}{\delta_j - \delta_{j+1}}\}, \tag{23}$$

where $\mathcal{I} = \{i | \delta_i > \delta_{i+1}, 1 \leq i \leq K-1\}$.

Furthermore, we discuss the relationship between the variables τ_t and ρ_D. By substituting (18) into (8), we have

$$0 \leq \tau_t \rho_D \leq \bar{D} - \bar{C}\tau_t, \tag{24}$$

where $\rho_D^e = \frac{p_D^e}{\sigma^2}$, $\rho_D^t = \frac{p_D^t}{\sigma^2}$, $\bar{C} = \rho_D^t - \rho_D^e + \eta\rho_B |h_{B,D_t}|^2$, and $\bar{D} = T\eta\rho_B |h_{B,D_t}|^2 - T\rho_D^e$. As $\rho_D^t > \rho_D^e$, we can conclude that $\bar{C} > 0$, and $\bar{D} - \bar{C}\tau_t$ decreases with τ_t.

Based on the above analysis, the resource optimization problem (17) is reduced to the following one

$$\max_{\tau_t, \rho_D} U_D = \tau_t \log_2(1 + \frac{|h_D|^2 \rho_D}{\bar{E}\rho_D + \bar{F}}), \tag{25a}$$

$$\text{s.t. (23), (24),} \tag{25b}$$

where $\bar{E} = \bar{A}|h_{B,D_r}|^2\rho_B$, and $\bar{F} = \bar{B}|h_{B,D_r}|^2\rho_B + 1$. In this problem (25), the variables ρ_D and τ_t are still deeply coupled. In the sequel, we discuss the optimal solution by dividing the feasible region of τ_t into two sub-intervals.

B. THE OPTIMAL SOLUTION TO PROBLEM (25)

First, the feasible conditions of problem (25) are provided.

Theorem 3: The optimization problem (25) is feasible if and only if $\bar{B} \leq 1$ and $\eta\rho_B |h_{B,D_t}|^2 \geq \rho_D^e$.

Proof: From Eq. (21), we have $\frac{1-\bar{B}}{\bar{A}} \geq 0$, and equivalently $\bar{B} \leq 1$. Meanwhile, from Eq. (24), we can conclude that $\bar{D} - \bar{C}\tau_t \geq 0$ should be strictly guaranteed. Hence, we should set $\bar{D} \geq 0$, namely $\eta\rho_B |h_{B,D_t}|^2 \geq \rho_D^e$. ∎

Next, the range of τ_t is divided into two intervals to simplify the constraint (25b). Combing (23) and (24), if $\bar{D} - \bar{C}\tau_t \geq \rho_D^{max}\tau_t$, namely $0 \leq \tau_t \leq \frac{\bar{D}}{\bar{C} + \rho_D^{max}}$, the constraint (25b) can be reduced as $0 \leq \rho_D \leq \rho_D^{max}$. Otherwise, if $0 \leq$

$\bar{D} - \bar{C}\tau_t \le \rho_D^{max}\tau_t$, namely $\frac{\bar{D}}{\bar{C}+\rho_D^{max}} \le \tau_t \le \frac{\bar{D}}{\bar{C}}$, the constraint (25b) becomes $0 \le \rho_D \le \frac{\bar{D}-\bar{C}\tau_t}{\tau_t}$. Hence, the optimal solution of (25) can be achieved in the following two cases:

1) CASE I ($0 \le \tau_t \le \frac{\bar{d}}{\bar{c}+\rho_d^{max}}$)

For this case, the constraint (25b) can be simplified as

$$0 \le \rho_D \le \rho_D^{max}, \quad 0 \le \tau_t \le \frac{\bar{D}}{\bar{C}+\rho_D^{max}}. \tag{26}$$

Referring to (25a), we can obtain that U_D increases with both ρ_D and τ_t. Therefore, the optimal solution of (25) can be easily achieved as $\rho_{D,1}^* = \rho_D^{max}$, $\tau_{t,1}^* = \frac{\bar{D}}{\bar{C}+\rho_D^{max}}$. The corresponding throughput of the D2D communication is $U_{D,1}^* = \tau_{t,1}^* \log_2(1 + \frac{|h_D|^2\rho_{D,1}^*}{\bar{E}\rho_{D,1}^*+\bar{F}})$.

2) CASE II ($\frac{\bar{d}}{\bar{c}+\rho_d^{max}} \le \tau_t \le \frac{\bar{d}}{\bar{c}}$)

For this case, the constraint (25b) can be reduced as

$$0 \le \rho_D \le \frac{\bar{D}-\bar{C}\tau_t}{\tau_t}, \quad \frac{\bar{D}}{\bar{C}+\rho_D^{max}} \le \tau_t \le \frac{\bar{D}}{\bar{C}}. \tag{27}$$

As U_D increases with ρ_D, we set the optimal $\rho_{D,2}^*$ as $\frac{\bar{D}-\bar{C}\tau_t}{\tau_t}$. Then the optimization problem (25) can be rewritten as

$$\max_{\tau_t} U_D(\tau_t) = \tau_t \log_2(\frac{m_1\tau_t + n_1}{m_2\tau_t + n_2}), \tag{28a}$$

$$\text{s.t. } \frac{\bar{D}}{\bar{C}+\rho_D^{max}} \le \tau_t \le \frac{\bar{D}}{\bar{C}}. \tag{28b}$$

where $m_1 = \bar{F} - \bar{C}\bar{E} - \bar{C}|h_D|^2$, $n_1 = \bar{D}\bar{E} + \bar{D}|h_D|^2$, $m_2 = \bar{F} - \bar{C}\bar{E}$, and $n_2 = \bar{D}\bar{E}$.

It is still difficult to obtain the closed-form optimal solution to (28) because the property of function $U_D(\tau_t)$ depends on the parameters (m_1, m_2, n_1 and n_2). In some cases as presented in the following theorems, the objective function $U_D(\tau_t)$ is either a concave one or monotone. Thus, the optimal solution of problem (28) can be easily found.

Theorem 4: If the parameters m_1, m_2, n_1 and n_2 satisfy one of the following two constraints, the function $U_D(\tau_t)$ is concave and the problem (28) becomes a convex optimization problem, whose optimal solution can be obtained by using mature algorithms: i) $m_1n_2 + m_2n_1 \ge 0$; ii) $m_1n_2 + m_2n_1 < 0$ and $\frac{\bar{D}(m_1n_2+m_2n_1)}{\bar{C}} + 2n_1n_2 \ge 0$.

Proof: See Appendix C. ∎

Theorem 5: Assuming that i)$\bar{F} - \bar{C}\bar{E} < 0$ ii) the circuit power consumption is small enough compared to the transmit power consumption, namely $\rho_D^e = \rho_D^t = 0$, we can derive that $U_D(\tau_t)$ in Eq. (28a) increases with τ_t, and the optimal solution is $\tau_{t,2}^* = \frac{\bar{D}}{\bar{C}}$.

Proof: See Appendix D. ∎

For the general cases, as the derivation of $U_D(\tau_t)$ with respect to τ_t exists, we can always find a sub-optimal solution by employing the gradient method [21], as shown in *Algorithm 1*. In this algorithm, ϵ is an accuracy control parameter, Δ is the step size, $G = \nabla U_D(x) = \frac{1}{\ln 2}\left[\ln(\frac{m_1 x+n_1}{m_2 x+n_2}) + x(\frac{m_1}{m_1 x+n_1} - \frac{m_2}{m_2 x+n_2})\right]$. Note that if there exists at most one saddle point for $U_D(\tau_t)$ in the interval $[\frac{\bar{D}}{\bar{C}+\rho_D^{max}}, \frac{\bar{D}}{\bar{C}}]$, the solution $\tau_{t,2}^*$ obtained from the *Algorithm 1* is indeed the optimal solution of the problem (28). Correspondingly, $\rho_{D,2}^* = \frac{\bar{D}-\bar{C}\tau_{t,2}^*}{\tau_{t,2}^*}$, and $U_{D,2}^* = \tau_{t,2}^* \log_2(1 + \frac{|h_D|^2\rho_{D,2}^*}{\bar{E}\rho_{D,2}^*+\bar{F}})$.

In summary, the optimal solution of (25) can be achieved as $(\rho_D^*, \tau_t^*) = \begin{cases} (\rho_{D,1}^*, \tau_{t,1}^*), & \text{if } U_{D,1}^*(\rho_{D,1}^*, \tau_{t,1}^*) \ge U_{D,2}^*(\rho_{D,2}^*, \tau_{t,2}^*) \\ (\rho_{D,2}^*, \tau_{t,2}^*), & \text{otherwise} \end{cases}$.

Algorithm 1 Searching for the Optimal Time Scheduling Parameter τ_t^*

Input:
$\{h_i, h_{D,i}, \gamma_i, i = 1, \cdots, K\}$, h_D, h_{B,D_t}, h_{B,D_r}, T, P_B, σ^2, η, p_D^t, p_D^e, Δ, ϵ;
Output:
τ_t^*;

```
Initialization: τ_t^p = D̄/(C̄+ρ_D^max) + ε, τ_t = D̄/(C̄+ρ_D^max);
Calculate m_1, m_2, n_1, and n_2;
while |τ_t − τ_t^p| ≥ ε do
    Set τ_t^p = τ_t;
    Calculate τ_t = τ_t^p + Δ * G;
    if τ_t > D̄/C̄ then
        Set τ_t = D̄/C̄;
    end if
    if τ_t < D̄/(C̄+ρ_D^max) then
        Set τ_t = D̄/(C̄+ρ_D^max);
    end if
end while
return τ_t^* = τ_t;
```

IV. THE OMA SCHEME

In this section, the conventional OMA scheme is investigated. For comparison, we adopt the orthogonal frequency division multiple access (OFDMA) system as the benchmark. As to the OFDMA scheme, a two-phase transmission framework is also introduced. The process for the first phase is same with that in the NOMA-based scheme, while for the second phase, the total bandwidth is equally divided into K units and each CU is only allowed to access single unit. Then the energy consumption constraint of the DTX can be expressed as

$$(T - \tau_t^o)p_D^e + \tau_t^o p_D^o + \tau_t^o p_D^t \le (T - \tau_t^o)\eta P_B |h_{B,D_t}|^2. \tag{29}$$

Furthermore, the SINR at the U_i and DRX during the second phase can be respectively calculated as

$$SINR_i^2 = \frac{\alpha_i^o |h_i|^2 \rho_B}{|h_{D,i}|^2\rho_D^o + 1}, \quad SINR_{D,i}^2 = \frac{|h_D|^2\rho_D^o}{(\sum_{i=1}^{K}\alpha_i^o)|h_{B,D_r}|^2\rho_B + 1}, \tag{30}$$

where α_i^o should satisfy

$$\sum_{i=1}^{K} \alpha_i^o \leq 1, \alpha_i^0 \geq 0, \forall i \in \mathcal{K}. \tag{31}$$

Correspondingly, the transmission rate of U_i during the second phase should be guaranteed, namely

$$R_i^2 = \frac{1}{K} \log_2(1 + SINR_i^2) \geq \gamma_i. \tag{32}$$

To maximize the achievable throughput of the DTX, the resource allocation problem can be formulated as

$$\max_{\boldsymbol{\alpha}^o, \rho_D^o, \tau_t^o} U_D = \tau_t^o R_{D,i}^2, \tag{33a}$$

$$\text{s.t. (29), (31), (32).} \tag{33b}$$

Similarly, by holding the equalities in the constraint (32), the problem (33) can be equally recast as

$$\max_{\tau_t^o, \rho_D^o} U_D = \tau_t^o log_2(1 + \frac{|h_D|^2 \rho_D^o}{\bar{E}^o \rho_D^o + \bar{F}^o}), \tag{34a}$$

$$0 \leq \tau_t^o \rho_D^o \leq \bar{D} - \bar{C}\tau_t^o, \tag{34b}$$

$$0 \leq \rho_D^o \leq \frac{1 - \bar{B}^o}{\bar{A}^o}. \tag{34c}$$

where $\phi_i^o = 2^{K\gamma_i} - 1$, $\bar{A}^o = \frac{\sum_{i=1}^{K} \phi_i^o \delta_i}{\rho_B}$, $\bar{B}^o = \frac{\sum_{i=1}^{K} \phi_i^o \theta_i}{\rho_B}$, $\bar{E}^o = \bar{A}^o |h_{B,Dr}|^2 \rho_B$, and $\bar{F}^o = \bar{B}^o |h_{B,Dr}|^2 \rho_B + 1$.

The problem (34) is similar to the problem (25), and the optimal solution of (34) can be achieved by applying the same algorithm analyzed in the NOMA-based scheme.

V. NUMERICAL RESULTS

In this section, numerical results are presented to evaluate the performance of our proposed NOMA-based scheme. The cell is a 100m×100m disc with BS being located in the center. The maximum distance between the D2D transmitter and receiver is 10m. Meanwhile, the channel is modeled as $h = gd^{-\frac{\beta}{2}}$, where g is the Rayleigh fading channel coefficient, d is the distance, and β is the path loss exponent. We assume that g follows complex normal distribution with zero mean and unit variance, namely $g \sim \mathcal{CN}(0, 1)$. The detailed system parameters setting are presented in Table 1. Note that all

TABLE 1. Simulation parameters.

Parameter	Value
D(radius of the disc)	$100\ m$
K(number of cellular users)	4
β(path loss exponent)	2
p_D^e(circuit power consumption for the energy-harvesting)	$5\ mW$
p_D^t(circuit power consumption for the transmitting)	$10\ mW$
σ^2(noise power)	$2 * 10^{-6}\ W$
P_B(BS's transmit power)	$2\ W$
η(energy transformation efficiency)	0.9
T(time of one frame)	$10\ s$
$\gamma_i = \gamma_{th}, \forall i \in \mathcal{K}$(rate requirement of CUs)	$0.1\ bps/Hz$
ϵ(accuracy control parameter)	10^{-7}
Δ(step size)	Backtracking line search

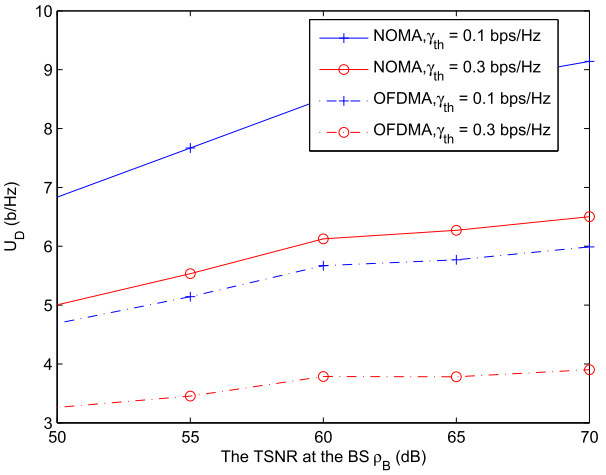

FIGURE 1. The relationship between U_D and ρ_B.

the numerical results are acquired by averaging over 10^6 realizations.

Fig. 1 investigates the relationship between the DTX's throughput U_D and the transmit SNR (TSNR) ρ_B. The observations are threefold. First, the throughputs U_D of both the NOMA and OFDMA schemes increases with ρ_B and decreases with γ_{th}, which can be easily explained as follows. From (23) and (24), a larger ρ_B and smaller γ_{th} expand the feasible range of the variable ρ_D, and thus leading to a higher throughput U_D. Second, the throughput U_D of the NOMA-based scheme is larger than that of the OFDMA scheme, which demonstrates the superiority of our proposed NOMA-based scheme over the traditional OMA scheme. The reason lies on that all the CUs and the D2D pair can share the entire spectrum resource for the NOMA-based scheme, which greatly improves the spectrum efficiency. Particularly, when $\rho_B = 70\ dB$ and $\gamma_{th} = 0.1\ bps/Hz$, our proposed NOMA-based scheme can achieve 50% throughput gain over the OFDMA scheme. Third, the throughput gap between the NOMA and OFDMA schemes increases with ρ_B. This means that the advantage of our proposed NOMA-based scheme is more obvious when the SNR ρ_B becomes larger.

Fig. 2 presents the curves of the throughput U_D vs γ_{th}. Similar to Fig. 1, the D2D throughput decreases with the SNR threshold γ_{th}, since the D2D transmit power should be lowered to reduce interference to the CUs in this case. Again, thanks to the advantage of NOMA, our proposed scheme can achieve 20% throughput gain over the OFDMA scheme especially when $\rho_B = 70\ dB$ and $\gamma_{th} = 0.6\ bps/Hz$.

Fig. 3 illustrates how the D2D throughput U_D changes with the number of CUs that share the same spectrum simultaneously. The throughputs of the two schemes both decrease with K, since the feasible region of the SNR at the D2D transmitter ρ_D becomes narrower when the number of CUs K increases. Furthermore, our proposed scheme outperforms the OFDMA scheme for $K \leq 5$, and is inferior to the OFDMA scheme for $K > 5$. The reason lies on that the scenario with large

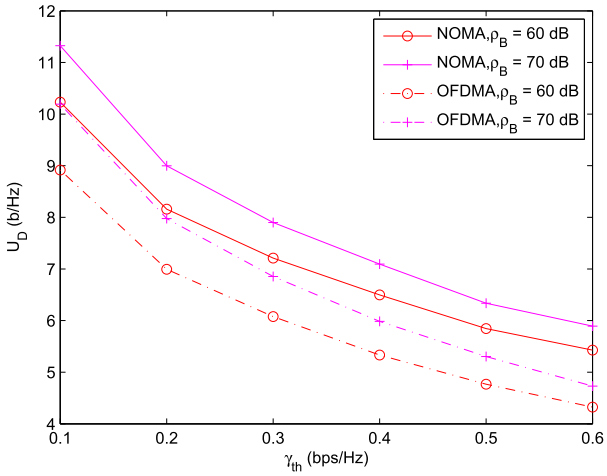

FIGURE 2. The relationship between U_D and γ_{th}.

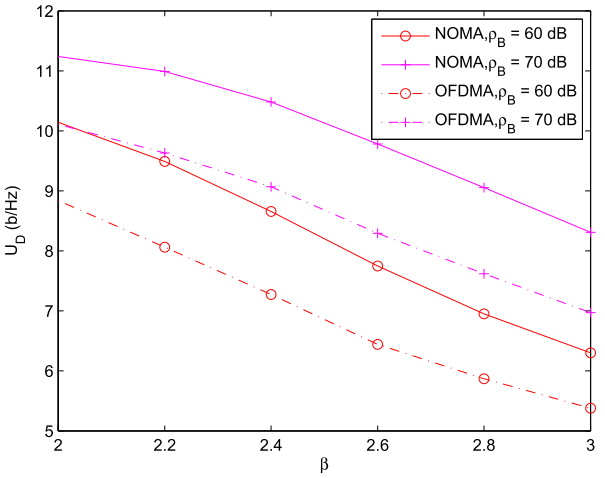

FIGURE 4. The relationship between U_D and β.

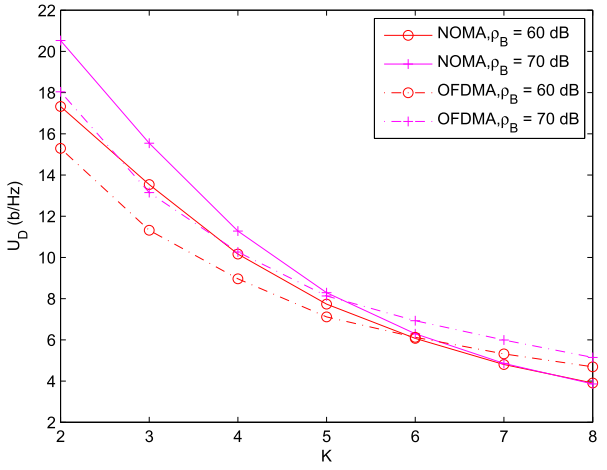

FIGURE 3. The relationship between U_D and K.

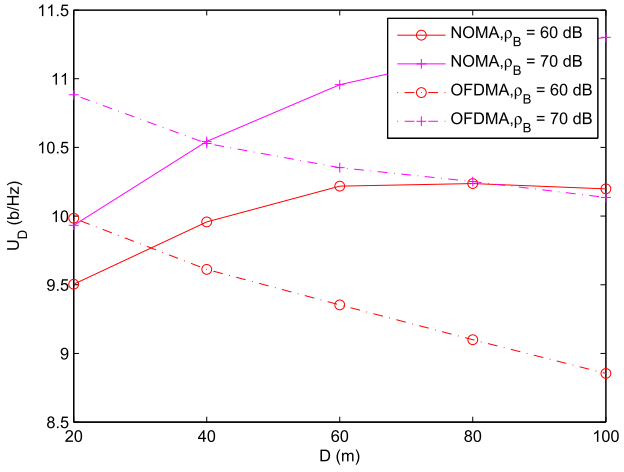

FIGURE 5. The relationship between U_D and D.

K is typically interference-limited while that with small K is bandwidth-limited. Thus, the OFDMA scheme achieves better performance due to the proper interference cancellation among the cellular users under the large K, and the NOMA-based scheme shows advantages under the small K due to the fact that all cellular users can share the entire spectrum resource.

Fig. 4 analyzes the relationship between the throughput U_D and β. It is easy to find that the throughputs of both two schemes decrease with β. As β gets large, the path loss becomes severe, leading to a small U_D. Meanwhile, our proposed NOMA-based scheme shows great advantages over the OFDMA scheme. In particular, when $\rho_B = 70\ dB$ and $\beta = 2$, the throughput of the NOMA-based scheme is almost 10 percentage higher than that of the OFDMA scheme.

Fig. 5 shows the relationship between the throughput U_D and D. A surprising observation is that the throughput of the NOMA-based scheme increases with D while that of the OFDMA scheme decreases with D, which can be explained as follows. The performance loss of large D results from the increasing path loss, and the performance gain of large D benefits from the interference decrement between the DTX and the CUs, and between the BS and the DRX. The interference decrement is dominated for the NOMA-based scheme while the path loss is dominated for the OFDMA scheme. Meanwhile, we can conclude that the NOMA-based scheme shows great advantages over the OFDMA scheme for $D \geq 40\ m$. Particularly, when $D = 100\ m$ and $\rho_B = 70\ dB$, the throughput of the NOMA-based scheme is nearly 10 percentage larger than that of the OFDMA scheme.

VI. CONCLUSION

In this paper, we have studied the resource optimization problem of a D2D underlaying NOMA-based cellular network with energy harvesting. The throughput of the D2D communication is maximized while the minimum rate requirement of each cellular user is guaranteed. We derived the optimal conditions for power control of cellular users and time allocation of energy harvesting, and achieved the optimal solution by solving the simplified optimization problem

under some cases. Otherwise, a suboptimal power control and time scheduling solution is found using a gradient-based algorithm. Simulation results show that our proposed NOMA-based scheme yields larger throughput than the corresponding OFDMA scheme.

APPENDIX A
PROOF OF THEOREM 1

First, the optimal solution of (17) satisfies $\tau_e^* + \tau_t^* = T$, which can be demonstrated by the contradiction method. Here we assume that $\tau_e^* + \tau_t^* < T$, and constraints (7), (8), (12), (16) are all guaranteed. Then we can construct a new solution $(\bar{\tau}_e,\bar{\tau}_t,\bar{\boldsymbol{\alpha}},\bar{p}_D)$ as $\bar{\tau}_e = \frac{T\tau_e^*}{\tau_e^*+\tau_t^*}$, $\bar{\tau}_t = \frac{T\tau_t^*}{\tau_e^*+\tau_t^*}$, $\bar{\boldsymbol{\alpha}} = \boldsymbol{\alpha}^*$, and $\bar{p}_D = p_D^*$. Therefore, it is easy to see $R_D^2(\bar{\boldsymbol{\alpha}}, \bar{p}_D) = R_D^2(\boldsymbol{\alpha}^*, p_D^*)$. From (17a), as $\bar{\tau}_t > \tau_t^*$, we can easily conclude that $U_D(\bar{\tau}_e, \bar{\tau}_t, \bar{\boldsymbol{\alpha}}, \bar{p}_D) > U_D(\tau_e^*, \tau_t^*, \boldsymbol{\alpha}^*, p_D^*)$, which contradicts our assumption.

Second, we show that the optimal solution of problem (17) satisfies (19). In the similar way, we assume that for the optimal solution $(\tau_e^*,\tau_t^*,\boldsymbol{\alpha}^*,p_D^*)$, constraints (1), (7), (8), (12) are all satisfied, and there exists at least one inequality in (16). Without loss of generality, we set $R_k^2(\boldsymbol{\alpha}^*, p_D^*) > \gamma_k$, and $R_i^2(\boldsymbol{\alpha}^*, p_D^*) \geq \gamma_i$, $i \in \mathcal{K}\backslash\{k\}$. Correspondingly, we construct a new solution $(\bar{\tau}_e,\bar{\tau}_t,\bar{\boldsymbol{\alpha}},\bar{p}_D)$ as $\bar{\tau}_e = \tau_e^*$, $\bar{\tau}_t = \tau_t^*$, $\bar{p}_D = p_D^*$, and $\bar{\alpha}_i = \alpha_i^*, \forall i \in \mathcal{K}\backslash\{k\}$, $\bar{\alpha}_k = \frac{(2^{\gamma_k}-1)(\sum_{j=1}^{k-1}\bar{\alpha}_j|h_k|^2\rho_B+|h_{D,k}|^2\rho_D+1)}{|h_k|^2\rho_B}$. Note that $R_k^2(\bar{\boldsymbol{\alpha}}, \bar{p}_D) = \gamma_k$. It is easy to find that $\bar{\alpha}_k < \alpha_k^*$, and thus $R_i^2(\bar{\boldsymbol{\alpha}}, \bar{p}_D) \geq R_i^2(\boldsymbol{\alpha}^*, p_D^*), \forall i \in \mathcal{K}$. Therefore, the solution $(\bar{\tau}_e,\bar{\tau}_t,\bar{\boldsymbol{\alpha}},\bar{p}_D)$ satisfies all the constraints. Similarly, since $\bar{\alpha}_k < \alpha_k^*$, we can conclude from Eq. (9) that $R_D^2(\bar{\boldsymbol{\alpha}}, \bar{p}_D) > R_D^2(\boldsymbol{\alpha}^*, p_D^*)$, and $U_D(\bar{\tau}_e, \bar{\tau}_t, \bar{\boldsymbol{\alpha}}, \bar{p}_D) > U_D(\tau_e^*, \tau_t^*, \boldsymbol{\alpha}^*, p_D^*)$, which contradicts our assumption that $(\tau_e^*,\tau_t^*,\boldsymbol{\alpha}^*,p_D^*)$ is the optimal solution.

The *Theorem 1* is completely proved.

APPENDIX B
PROOF OF THEOREM 2

The constraint (19) can be further simplified as

$$\frac{\rho_B\alpha_i}{\sum_{j=1}^{i-1}\rho_B\alpha_j + \delta_i\rho_D + \theta_i} = \phi_i, \quad \forall i \in \mathcal{K}, \tag{35}$$

where $\phi_i = 2^{\gamma_i} - 1$, $\delta_i = \frac{|h_{D,i}|^2}{|h_i|^2}$, $\theta_i = \frac{1}{|h_i|^2}$, and $\sum_{j=1}^{i-1}\rho_B\alpha_j = 0$ for $i-1 < j$. Then α_1 can be easily obtained as

$$\alpha_1 = \frac{\phi_1(\delta_1\rho_D + \theta_1)}{\rho_B}. \tag{36}$$

As to $U_i, i \in \mathcal{K}\backslash\{1\}$, α_i can be given by

$$\alpha_i = \frac{\phi_i(\sum_{j=1}^{i-1}\alpha_j\rho_B + \delta_i\rho_D + \theta_i)}{\rho_B}, \quad i \in \mathcal{K}\backslash\{1\}. \tag{37}$$

Then, we define $S_i = \sum_{j=1}^{i}\alpha_j\rho_B$. A recursive expression of S_i can be obtained from (37)

$$\begin{aligned} S_i &= S_{i-1} + \alpha_i\rho_B = S_{i-1} + \phi_i(S_{i-1} + \delta_i\rho_D + \theta_i) \\ &= (1+\phi_i)S_{i-1} + \phi_i(\delta_i\rho_D + \theta_i) \\ &= \left[\prod_{j=2}^{i}(1+\phi_j)\right] S_1 \\ &\quad + \sum_{j=2}^{i}\left\{\left[\prod_{t=j+1}^{i}(1+\phi_t)\right]\phi_j(\delta_j\rho_D + \theta_j)\right\} \\ &= \sum_{j=1}^{i}\left\{\left[\prod_{t=j+1}^{i}(1+\phi_t)\right]\phi_j(\delta_j\rho_D + \theta_j)\right\}, \end{aligned} \tag{38}$$

where the last equality comes from that $S_1 = \phi_1(\delta_1\rho_D + \theta_1)$, and $\prod_{t=j+1}^{i}(1+\phi_t) = 1$ for $j+1 > i$. Therefore, $\alpha_i = \frac{S_i - S_{i-1}}{\rho_B}$ $(i \geq 2)$ can be calculated as

$$\alpha_i = \frac{\sum_{j=1}^{i-1}\left\{\left[\prod_{t=j+1}^{i-1}(1+\phi_t)\right]\phi_i\phi_j(\delta_j\rho_D + \theta_j)\right\} + \phi_i(\delta_i\rho_D + \theta_i)}{\rho_B}, \tag{39}$$

where $i \geq 2$ and $\prod_{t=j+1}^{i-1}(1+\phi_t) = 1$ for $j+1 > i-1$.

Referring to (36) and (39), the optimal $\boldsymbol{\alpha}^*$ can be represented by (20), and *Theorem 2* is completely proved.

APPENDIX C
PROOF OF THEOREM 4

The second derivative of $U_D(\tau_t)$ with respect to τ_t can be calculated as

$$\nabla^2 U_D(\tau_t) = \frac{(m_1n_2 - m_2n_1)[(m_1n_2 + m_2n_1)\tau_t + 2n_1n_2]}{(m_1\tau_t + n_1)^2(m_2\tau_t + n_2)^2}. \tag{40}$$

By substituting m_1, n_1, m_2, n_2, the expression $m_1n_2 - m_2n_1$ can be further derived as $m_1n_2 - m_2n_1 = -\bar{D}\bar{F}|h_D|^2$. Since $\bar{D} > 0$, $\bar{F} > 0$, and $|h_D|^2 > 0$, we can obtain that $m_1n_2 - m_2n_1 < 0$.

The concavity of $U_D(\tau_t)$ can be analyzed as follows. First, if $m_1n_2 + m_2n_1 \geq 0$, as $n_1 > 0$, $n_2 > 0$ and $\tau_t > 0$, the expression $(m_1n_2 + m_2n_1)\tau_t + 2n_1n_2$ is greater than zero, and $\nabla^2 U_D(\tau_t) < 0$. Second, if $m_1n_2 + m_2n_1 < 0$, as $\frac{\bar{D}}{\bar{C}+\rho_D^{max}} \leq \tau_t \leq \frac{\bar{D}}{\bar{C}}$, we can find that $\nabla^2 U_D(\tau_t) \leq 0$ for any τ_t when $\frac{\bar{D}(m_1n_2+m_2n_1)}{\bar{C}} + 2n_1n_2 \geq 0$.

In summary, if m_1, m_2, n_1 and n_2 satisfy one of the following two constraints, the function $U_D(\tau_t)$ is concave: i) $m_1n_2 + m_2n_1 \geq 0$; ii) $m_1n_2 + m_2n_1 < 0$ and $\frac{\bar{D}(m_1n_2+m_2n_1)}{\bar{C}} + 2n_1n_2 \geq 0$.

APPENDIX D
PROOF OF THEOREM 5

When $\rho_D^e = \rho_D^t = 0$, we can obtain that $m_1 = \bar{F} - \bar{C}(\bar{E} + |h_D|^2)$, $n_1 = \bar{D}(\bar{E} + |h_D|^2)$, $m_2 = \bar{F} - \bar{C}\bar{E}$, and $n_2 = \bar{D}\bar{E}$. Note that $n_1 > 0$, and $n_2 > 0$.

Define $s_1 = \frac{n_1}{m_1}$, $s_2 = \frac{n_2}{m_2}$, and $z = \frac{m_1}{m_2}$. As $\bar{F} - \bar{C}\bar{E} < 0$, we have $m_1 < m_2 < 0$. Meanwhile, we can find that $n_1 m_2 - n_2 m_1 = \bar{D}\bar{F}|h_D|^2 > 0$. Correspondingly, the following inequalities can be derived as

$$z > 1, \quad s_1 < s_2 < 0. \tag{41}$$

Then $\nabla_{\tau_t} U_D(\tau_t)$ can be calculated as

$$\begin{aligned}
&\nabla_{\tau_t} U_D(\tau_t) \\
&= \frac{1}{\ln 2} \nabla_{\tau_t} \left[\tau_t \ln(z \frac{\tau_t + s_1}{\tau_t + s_2}) \right] = \frac{\ln z}{\ln 2} \\
&\quad + \frac{1}{\ln 2} \Bigg\{ \underbrace{\left[\ln(\tau_t + s_1) - \frac{s_1}{\tau_t + s_1} \right] - \left[\ln(\tau_t + s_2) - \frac{s_2}{\tau_t + s_2} \right]}_{\mathcal{L}_1} \Bigg\}.
\end{aligned} \tag{42}$$

Define $Q(s) = \ln(\tau + s) - \frac{s}{\tau + s}$, $s < 0$. Deriving $Q(s)$ with respect to s, we can see that

$$\nabla_s Q(s) = \frac{s}{(\tau + s)^2} < 0, \quad s < 0. \tag{43}$$

Hence, $Q(s)$ decreases with s for $s < 0$. Correspondingly, $\mathcal{L}_1 > 0$ and $\ln z > 0$. We can conclude that $\nabla_{\tau_t} U_D(\tau_t) > 0$, and $U_D(\tau_t)$ increases with τ_t. Therefore, the optimal solution of (28) is $\tau_{t,2}^* = \frac{\bar{D}}{\bar{C}}$, and $\rho_{D,2}^* = \frac{\bar{D} - \bar{C}\tau_{t,2}^*}{\tau_{t,2}^*} = 0$.

REFERENCES

[1] K. Doppler, M. Rinne, C. Wijting, C. Ribeiro, and K. Hugl, "Device-to-device communication as an underlay to LTE-advanced networks," *IEEE Commun. Mag.*, vol. 47, no. 12, pp. 42–49, Dec. 2009.
[2] G. Fodor *et al.*, "Design aspects of network assisted device-to-device communications," *IEEE Commun. Mag.*, vol. 50, no. 3, pp. 170–177, Mar. 2012.
[3] J. Liu, Y. Kawamoto, H. Nishiyama, N. Kato, and N. Kadowaki, "Device-to-device communications achieve efficient load balancing in LTE-advanced networks," *IEEE Wireless Commun. Mag.*, vol. 21, no. 2, pp. 57–65, Feb. 2014.
[4] X. Lin, J. G. Andrews, and A. Ghosh, "Spectrum sharing for device-to-device communication in cellular networks," *IEEE Trans. Wireless Commun.*, vol. 13, no. 12, pp. 6727–6740, Dec. 2014.
[5] C.-H. Yu, O. Tirkkonen, K. Doppler, and C. Ribeiro, "On the performance of device-to-device underlay communication with simple power control," in *Proc. VTC*, Apr. 2009, pp. 1–5.
[6] J. Wang, D. Zhu, C. Zhao, J. C. F. Li, and M. Lei, "Resource sharing of underlaying device-to-device and uplink cellular communications," *IEEE Commun. Lett.*, vol. 17, no. 6, pp. 1148–1151, Jun. 2013.
[7] D. Feng, L. Lu, Y. Yuan-Wu, G. Y. Li, G. Feng, and S. Li, "Device-to-device communications underlaying cellular networks," *IEEE Trans. Commun.*, vol. 61, no. 8, pp. 3541–3551, Aug. 2013.
[8] S. M. R. Islam, N. Avazov, O. A. Dobre, and K.-S. Kwak, "Power-domain non-orthogonal multiple access (NOMA) in 5G systems: Potentials and challenges," *IEEE Commun. Surveys Tuts.*, vol. 19, no. 2, pp. 721–742, 2nd Quart., 2017.
[9] Z. Ding, X. Lei, G. K. Karagiannidis, R. Schober, J. Yuan, and V. Bhargava, "A survey on non-orthogonal multiple access for 5G networks: Research challenges and future trends," *IEEE J. Sel. Areas Commun.*, vol. 35, no. 10, pp. 2181–2195, Oct. 2017.
[10] Y. Saito, A. Benjebbour, Y. Kishiyama, and T. Nakamura, "System-level performance evaluation of downlink non-orthogonal multiple access (NOMA)," in *Proc. IEEE Annu. Symp. Pers., Indoor, Mobile Radio Commun. (PIMRC)*, London, U.K., Sep. 2013, pp. 611–615.
[11] Z. Ding, Z. Yang, P. Fan, and H. V. Poor, "On the performance of non-orthogonal multiple access in 5G systems with randomly deployed users," *IEEE Signal Process. Lett.*, vol. 21, no. 12, pp. 1501–1505, Dec. 2014.
[12] S. Timotheou and I. Krikidis, "Fairness for non-orthogonal multiple access in 5G systems," *IEEE Signal Process. Lett.*, vol. 22, no. 10, pp. 1647–1651, Oct. 2015.
[13] Z. Yang, Z. Ding, P. Fan, and N. Al-Dhahir, "A general power allocation scheme to guarantee quality of service in downlink and uplink NOMA systems," *IEEE Trans. Wireless Commun.*, vol. 15, no. 11, pp. 7244–7257, Nov. 2016.
[14] Z. Zhang, Z. Ma, M. Xiao, Z. Ding, and P. Fan, "Full-duplex device-to-device-aided cooperative nonorthogonal multiple access," *IEEE Trans. Veh. Technol.*, vol. 66, no. 5, pp. 4467–4471, May 2017.
[15] J. Zhao, Y. Liu, K. K. Chai, Y. Chen, and M. Elkashlan, "Joint subchannel and power allocation for NOMA enhanced D2D communications," *IEEE Trans. Commun.*, vol. 65, no. 11, pp. 5081–5094, Nov. 2017.
[16] J.-B. Kim, I.-H. Lee, and J.-H. Lee, "Capacity scaling for D2D aided cooperative relaying systems using NOMA," *IEEE Commun. Lett.*, vol. 7, no. 1, pp. 42–45, Feb. 2018.
[17] Y. Pan *et al.*, "Resource allocation for D2D communications underlaying a NOMA-based cellular network," *IEEE Wireless Commun. Lett.*, vol. 7, no. 1, pp. 130–133, Feb. 2018.
[18] H. Wang *et al.*, "Resource allocation for energy harvesting-powered D2D communications underlaying cellular networks," in *Proc. IEEE Int. Conf. Commun.*, May 2017, pp. 1–6.
[19] L. Pei *et al.*, "Energy-efficient D2D communications underlaying NOMA-based networks with energy harvesting," *IEEE Commun. Lett.*, vol. 22, no. 5, pp. 914–917, Mar. 2018.
[20] W. Dinkelbach, "On nonlinear fractional programming," *Manage. Sci.*, vol. 13, no. 7, pp. 492–498, Mar. 1967.
[21] S. Boyd and L. Vandenberghe, *Convex Optimization*. Cambridge, U.K.: Cambridge Univ. Press, 2004.

BO CHEN received the B.Eng. and Ph.D. degrees in information science and electrical engineering from Zhejiang University, China, in 2011 and 2016, respectively. Since 2016, he has been a Lecturer with the Faculty of Electrical Engineering and Computer Science, Ningbo University, China. His current research interests include non-orthogonal multiple access (NOMA), unmanned aerial vehicle (UAV), and other 5G related topics.

JUAN LIU (M'15) received the Ph.D. degree in electronic engineering from Tsinghua University, Beijing, China, in 2011.

From 2012 to 2014, she was a Postdoctoral Research Scholar with the Department of Electrical and Computer Engineering, NC State University (NCSU), Raleigh, NC, USA. From 2015 to 2016, she was a Research Associate with the Department of Electronic and Computer Engineering, The Hong Kong University of Science and Technology (HKUST), Hong Kong. Since 2016, she has been with the College of Information Science and Engineering, Ningbo University, Ningbo, China, where she is currently an Associate Professor. Her research interests include wireless communications, and distributed signal processing and networking. She is focusing on the topics on wireless caching, mobile edge computing, and distributed inference for large-scale networks. She has served as a TPC Member for IEEE ICC 2010, ICC 2012, ICC 2014, and GLOBECOM Workshop 2016. She and her co-workers received the Best Paper Award in IEEE ICC 2016. She has also served as a reviewer for the IEEE journals including the IEEE JSAC, TCOM, TSP, TVT, and WCL, and the IEEE conferences including IEEE INFOCOM, ICC, GLOBECOM, WCNC, and VTC. She is an Associate Editor of the IEEE Access.

XINJIE YANG received the B.S. and M.S. degrees in telecommunications engineering from the Beijing University of Posts and Telecommunications, Beijing, China, in 1993 and 1998, respectively, and the Ph.D. degree in mobile communications from the University of Surrey, Surrey, U.K., in 2003, where he was a Research Fellow with the Center for Communication Systems Research, from 2001 to 2005. From 2006 to 2017, he was with NEC Europe Ltd., London, U.K., serving a number of different positions, such as the Senior Product Manager, the Manager of Product Line Management, and the Manager of Technical Marketing. Since 2017, he has been with Ningbo University, Ningbo, China, where he is currently a Full Professor. His main research interests are next generation mobile network architecture and the cellular IoT networks.

LINGFU XIE received the B.Eng. and M.Eng. degrees in communications engineering from the University of Electronic Science and Technology of China, in 2006 and 2009, respectively, and the Ph.D. degree from Nanyang Technological University, Singapore, in 2014. From 2014 to 2015, he was a Postdoctoral Fellow with The Hong Kong Polytechnic University, Hong Kong. In 2015, he joined the Faculty of Electrical Engineering and Computer Science, Ningbo University, Ningbo, China. His research interests mainly include protocol design and performance analysis in mobile networks, wireless network coding, and physical-layer network coding.

YOUMING LI received the B.S. degree in computational mathematics from Lanzhou University, China, in 1985, the M.S. degree in computational mathematics from Xian Jiaotong University, Xi'an, China, in 1988, and the Ph.D. degree in electrical Engineering from Xidian University, Xi'an, in 1995, where he was an Associate Professor with the Department of Applied Mathematics, from 1988 to 1998. From 1999 to 2004, he was with the School of Electrical and Electronics Engineering, Nanyang Technological University, DSO National Laboratories, Singapore, and the School of Engineering, Bar-Ilan University, Israel, respectively. Since 2005, he has been with Ningbo University, Ningbo, China, where he is currently a Professor. His research interests include cognitive radio and wireless/wireline communications.